Science of the Total Environment 628–629 (2018) 233–240

Contents lists available at ScienceDirect

Science of the Total Environment

journal homepage: www.elsevier.com/locate/scitotenv

Extreme weather impacts on tropical mangrove forests in the Eastern Brazil Marine Ecoregion

Ricardo Nogueira Servino, Luiz Eduardo de Oliveira Gomes *, Angelo Fraga Bernardino

Grupo de Ecologia Bêntica, Departamento de Oceanografia e Ecologia, Universidade Federal do Espírito Santo, Av. Fernando Ferrari, 514, Goiabeiras, Vitória, ES, 29075-910, Brazil

HIGHLIGHTS

- Over 24% of mangroves were suddenly lost by a hailstorm in Eastern Brazil.
- There was further degradation of impacted areas one year after the initial impact.
- *Rhizophora mangle* was the most impacted species by the hailstorm.
- Extreme weather events and long-term stress offer significant risks to wetlands.
- Significant economic social losses continue in the impacted estuary.

GRAPHICAL ABSTRACT

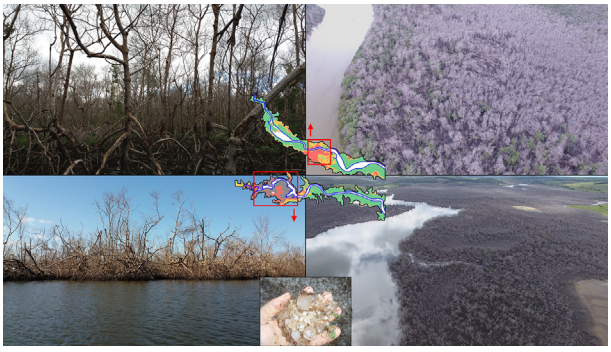

ARTICLE INFO

Article history:
Received 21 October 2017
Received in revised form 6 February 2018
Accepted 6 February 2018
Available online 13 February 2018

Editor: Elena PAOLETTI

Keywords:
El Niño
Hailstorm
Remote sensing
Mangrove
Climate change
Eastern Brazil

ABSTRACT

Extreme weather events are likely to become more frequent in the 21st century bringing significant impacts to coastal ecosystems. However, the capacity to detect and measure those impacts are still limited, with effects largely unstudied. In June 2016, a hailstorm with wind gusts of over 100 km·h^{-1} caused an unprecedented mangrove dieback on Eastern Brazil. To quantify the scale of impact and short-term recovery of mangroves (15-mo), we used satellite imagery and field sampling to evaluate changes in forest structure in control and impacted areas after the hailstorm. Satellite imagery revealed mangrove dieback in over 500 ha, corresponding to 29.3% of the total forest area suddenly impacted after the hailstorm. Fifteen months after the hailstorm, some impacted areas show an initial recovery, while others continued to degrade. The El Niño years of 2014–2016 created mild drought conditions in Eastern Brazil. As observed in wetlands of semi-arid regions during the same period, mangrove recovery may have been impaired by continued physiological stress and climate change effects. Economic losses in the study site from typical mangrove ecosystem services including food provision, climate regulation, raw materials and nurseries are estimated to at least US$ 792,624 yr^{-1}. This is the first evidence of an extreme weather impact on mangroves in Brazil that typically provide unique ecological and economic subsistence to coastal populations. Our results reveal that there is a pressing need for long-term monitoring and climate change adaptation actions for coastal wetlands in Brazil, and to provide broad estimates of ecosystem values associated with these ecosystems given many areas are already experiencing chronic stress from local impacts, drought and high temperatures.

* Corresponding author.
E-mail address: luiz.e.o.gomes@gmail.com (L.E.O. Gomes).

https://doi.org/10.1016/j.scitotenv.2018.02.068
0048-9697/

1. Introduction

Climate change is likely to impact coastal ecosystems through changes to mean temperatures, rainfall patterns and sea level along with alterations to the frequency and intensity of extreme events (IPCC, 2001; Doney et al., 2012). Sea level rise and regional changes in precipitation are of special concern for mangrove forests, which also need to cope with a naturally harsh estuarine environment (Alongi, 2008). Recent studies show that changes in minimum winter temperature and precipitation regimes are among the major climatic factors that may expand or contract coastal wetland ecosystem extensions in the future (Gabler et al., 2017; Feher et al., 2017; Osland et al., 2017). Concerningly, a marked decrease in precipitation volume and an increase in drought periods have already been observed in a number of coastal areas during the last few decades (Dai, 2013). Prolonged drought stress has been associated with massive losses of coastal wetlands including salt marshes and mangroves (McKee et al., 2004; Duke et al., 2017). Because mangrove forests are resilient to multiple environmental changes and human impacts, it has been difficult to identify causes of sudden massive dieback of marshes and mangrove trees; these events have been associated with long-term stress on vegetation by sea level and drought (Cintrón et al., 1978; Houston, 1999; Alongi, 2008).

There are over 960,000 ha of mangrove forests along the Brazilian coast distributed from the Amazon to subtropical Marine Ecoregions with variable climatic and geomorphological settings (Giri et al., 2010; Schaeffer-Novelli et al., 2016). Climate models and decadal climate trends indicate that most Marine Ecoregions in Brazil with extensive mangrove forests are under rising temperatures and are likely experiencing drought stress (Marengo et al., 2010; Dai, 2013; Bernardino et al., 2015). Given the importance of mangroves to climate regulation, fisheries and social resources, it is imperative to identify their vulnerability to long-term changes (e.g. high temperatures, sea-level rise and prolonged drought) before subtle and large-scale ecosystem losses occur, a challenge in most coastal areas given insufficient monitoring (Kristensen et al., 2008; Donato et al., 2011; Mcleod et al., 2011; Alongi, 2012; Queiroz et al., 2017). For example, based on the increase in frequency and intensity of extreme events in the 21 century (IPCC, 2001), El Niño can intensify the reduction in rainfall rates and increase evapotranspiration, impacting mangroves and marshes through physiological stress from salinization (MacKay et al., 2010; Allen et al., 2015; Brimelow et al., 2017).

Potential impacts of storms and hurricanes on mangrove forests are known to cause acute and long-term changes (Houston, 1999; Cahoon et al., 2003; McLeod and Salm, 2006; Long et al., 2016). Although episodic storms may lead to regional losses of mangrove forests, there is limited understanding of the potential damage that extreme weather events cause in forests experiencing chronic climate change stress. On June 1st, 2016, a hailstorm with wind gusts of 100 $km \cdot h^{-1}$ hit the mangrove forests of the Piraquê Açú-Mirím (PAM) estuary in Eastern Brazil. The hail event caused housing and infrastructure damage to the nearby villages of Santa Rosa (19.927°S, 40.284°W) and Irajá (19.905°S, 40.234°W). This was the first occurrence of an extreme weather event in the PAM estuary, which has 1746 ha of preserved mangrove forests within a conservation unit in the Eastern Brazil Marine ecoregion (Bernardino et al., 2015).

Monitoring coastal landscapes is a challenge that has greatly benefited from remote sensing techniques (Ibharim et al., 2015). Initiatives such as the Landsat Program offer high spatial and temporal resolution data to monitor climate conditions for long periods (Jones, 2015). In particular, vegetation indexes derived from satellite images are largely used to assess coastal impacts over large areas (Pettorelli, 2013; Yengoh et al., 2015; Duke et al., 2017). Here we used satellite images of the PAM estuary (Supplemental Fig. S1) to quantify the initial impact of an extreme weather event on mangrove forests in Eastern Brazil. We used images from three periods (pre-impact, impact and one year after impact) to assess changes in mangrove forest canopy; we attempted to identify the spatial scales of impact and study the temporal recovery of impacted sites. We finally assessed potential economic losses based on the spatial and temporal impacts on mangrove ecosystem services in the study area. This is the first evidence of a mangrove forest dieback suddenly driven by a hailstorm in Eastern Brazil, with little evidence of recovery one year after the event.

2. Materials and methods

2.1. Study area and sample design

The study area was located in the PAM estuary (17°58′S; 40°00′W), within the Eastern Brazil Marine Ecoregion (Bernardino et al., 2015; Fig. 1). The region has two well-defined seasons, dry winter (April to September) and wet summer (October to March), with an average rainfall of 111.1 ± 25.2 $mm \cdot y^{-1}$, temperatures of 24 to 26 °C (Alvares et al., 2013; Bernardino et al., 2015) and a semi-diurnal microtidal regime (<2 m). This estuary has a Y-shape morphology with 1746 ha of mangrove forests, composed of *Rhizophora mangle, Laguncularia racemosa* and *Avicennia schaueriana* (PMA, 2013). Water salinity in the PAM estuary ranges from 15.5 to 36 psu (Supplemental Fig. S2). A polyhaline sector is typically observed within the estuary as is a euhaline sector near the sea. The most recent in-situ monitoring of water salinity within the PAM estuary in Nov 2015 recorded salinities ranging from 34.6 to 39.1 psu. The PAM estuary is part of the municipal conservation unit: the "sustainable development reserve of the mangroves of the rivers Piraquê Açú and Piraquê Mirím". Traditional communities, such as fisherman and Tupinikin and Guarani indians, live near the estuary and use the fisheries resources (e.g. fishes and crabs) for subsistence. Other ecosystems services provided by PAM estuary are raw materials, tourism, climate regulation and nursery habitats. From 2014 to 2016, the PAM estuary was under the most intense El Niño of this century (ggweather, 2017), which resulted in decreased rainfall and salinization in the area (Fig. 2; Supplemental Fig. S2). After the hailstorm (June 1st 2016), a sudden massive dieback occurred along the fringe of the mangrove, classified as predominantly "moderate impact" in both areas (Piraquê Mirím = PM and Piraquê Açú = PA).

The impacts of the sudden hailstorm on mangrove forests were studied using a BACI design (before-versus-after, Underwood, 1992) by comparing satellite images of mangroves coverage before and after the hailstorm. Initial mangrove coverage was assessed from images collected up to one year before the hailstorm (Jan 2015 to May 2016). Impacted areas were assessed from images collected 1-mo to over 1-yr after the hailstorm (Jun 2016 to Aug, 2017). As the hailstorm impacted two sites within the PAM estuary, we monitored changes in those two sites near Irajá village (site PA) and Santa Rosa village (site PM). The spatial differences between impacted and natural mangrove forests were then compared with two control sites. The structure of mangrove forests in the PAM estuary was accessed at each control and impacted site after the hailstorm (August of 2017).

2.2. Weather assessment

Changes in rainfall patterns from 1948 to 2016 were monitored from automatic meteorological stations located in the nearest areas of the PAM estuary from the Brazil National Weather Agency (total daily rainfall; ANA, 2017, stations 1940002, 1940021 and 2549007). The standardized precipitation index (SPI) quantify the rainfall deficit, being useful to identify and monitor climatic droughts by categories, which range from ≥2 SPI to ≤−2 SPI (extreme wetness to extreme dryness; Supplemental Table S1; McKee et al., 1993). SPI can be calculated in a range of temporal scales (3 to 48-months scale), where 12-months scale is useful to identify climatic drought influence on hydrologic regimes and water resources (Moreira et al., 2008). The hailstorm was identified by the change in wind field patterns considering the intensity

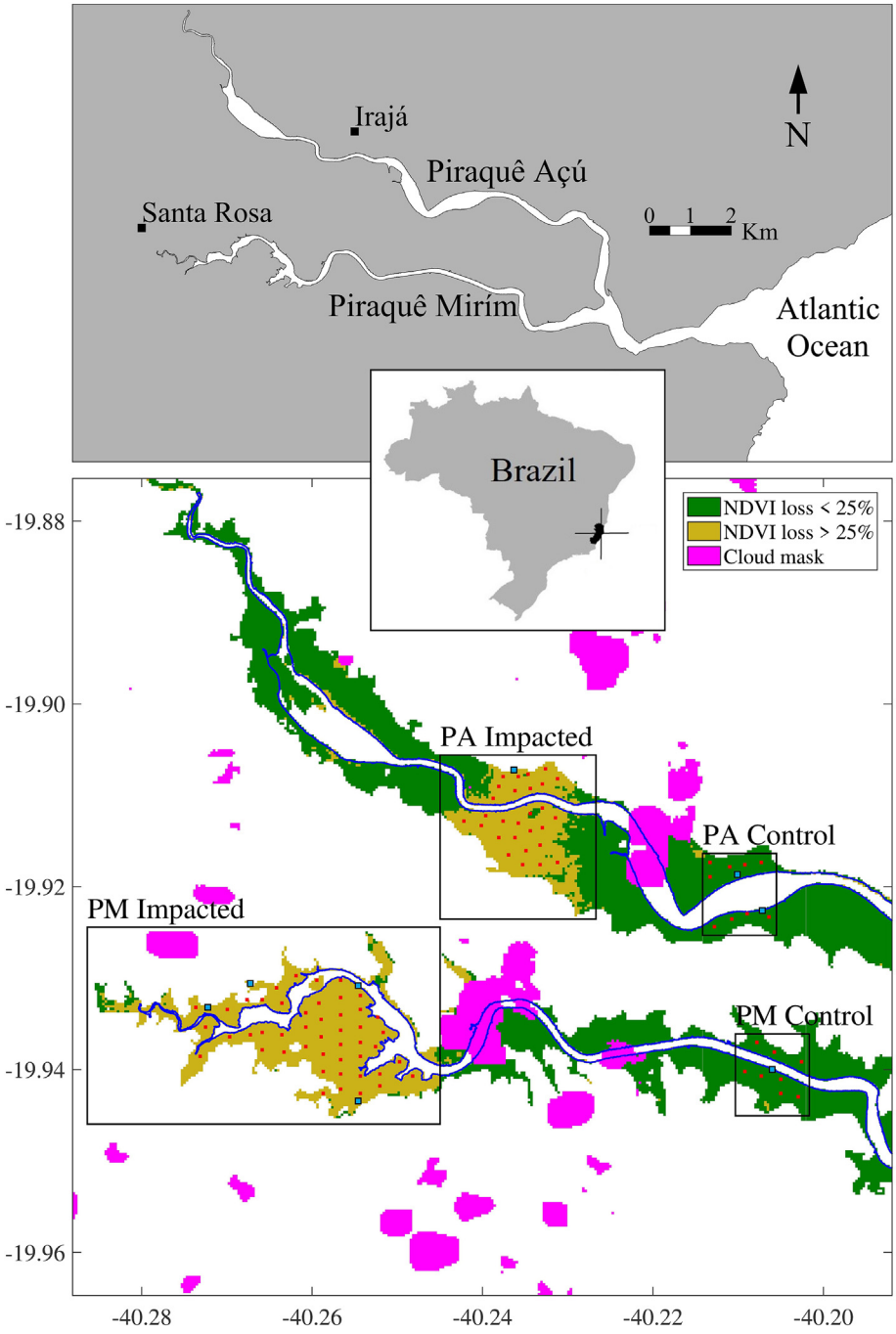

Fig. 1. Map indicating the impacted and control sites in the study area, including the Piraquê Açú (PA) and Piraquê-Mirím (PM) estuaries. NDVI changes were measured within each of the sites (red dots) before and after the hail storm.

of the decomposed zonal (u; positive to E) and meridional winds (v; positive to N). Estimates of "u" and "v" were acquired from the NCEP/NCAR database (Kalnay et al., 1996) at resolutions of 4 h and 2.5° latitude × 2.5° longitude. Local estimates were averaged from 19.8° to 20°S and 39.9° to 40.3°W and regional estimates were averaged from 17° to 22°S and 36° to 44°W.

2.3. Remote sensing and GIS

Mangrove loss was estimated at a landscape scale by remote sensing images from the Landsat 8 Operational Land Imager (U.S. Geological Survey, 2017a). Spatial resolution per pixel was 30 m. Although the satellite remaps the region every 8 days, time resolution is lower in practice and irregular due to the presence of clouds. Eighty-nine Level-1 images were downloaded after a visual pre-selection based on overall cloud coverage, depicting the study region from Jan 2015 to Nov 2017 (Supplemental Table S2). Visualization and processing of remote sensing data was performed using Matlab 9.0 (*MATLAB 9.0*, 2016) software.

Delimitation of the mangrove forests in the PAM estuary was carried manually using the shortwave infrared band (SWIR 1), as mangrove forests have a distinguishable lower reflectance in this band compared to surrounding terrestrial vegetation due to moisture content (Tamura and Kikushima, 2008). The satellite images were transformed into a Normalized Difference Vegetation Index (NDVI; Rouse et al., 1974) format. NDVI is arguably the most utilized vegetation index for scientific

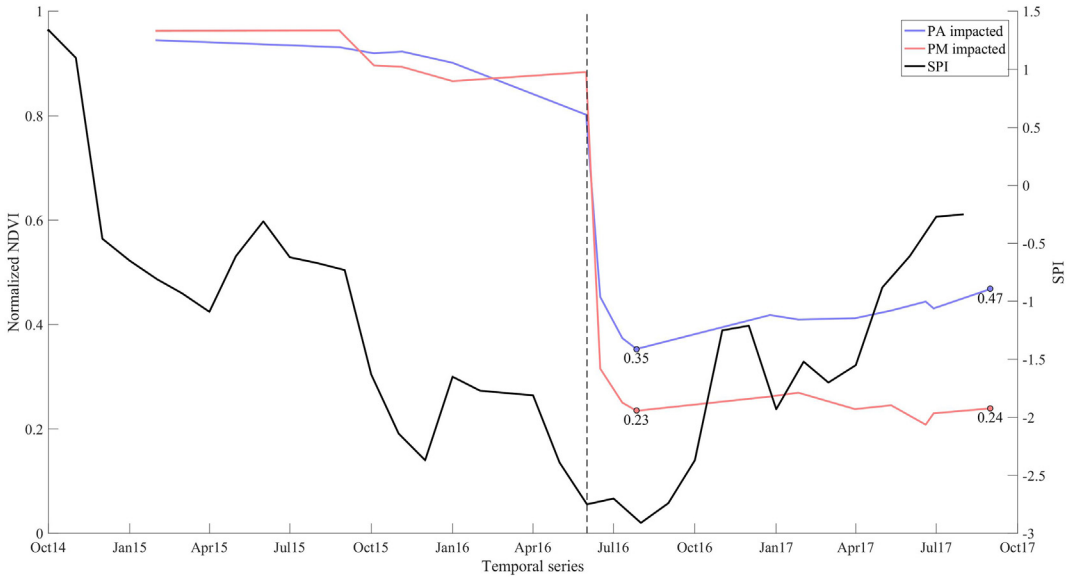

Fig. 2. Normalized NDVI values of impacted sites at the Piraquê-Açu (PA) and Piraquê-Mirim (PM) estuaries before and after the storm (June 2016, dashed black line). The Standard Precipitation Index (SPI, see methods) is indicated throughout the study period for the region.

research, used as a proxy for overall 'greenness' (Pettorelli, 2013). It was calculated using the formula:

$$\mathrm{NDVI} = \frac{\mathrm{NIR} - \mathrm{RED}}{\mathrm{NIR} + \mathrm{RED}}$$

where NIR is the near-infrared band and RED is the red band of spectral reflectance measurements.

Cloudy pixels were identified and masked with the Landsat 8 Pre-Collection Quality Assessment Band. Visual inspection was also needed, as pixel quality accuracy is <80% (U.S. Geological Survey, 2017b). Cloud-contaminated pixels can significantly decrease NDVI values (Holben, 1986), so images that had cloud influence over the regions of interest were discarded.

The impacted sites were selected and identified as a continuous area which suffered at least 25% NDVI loss immediately after the hailstorm. This was done using a comparison between images taken 1-day before (May, 31st 2016) and 15 days after the hailstorm (June, 16th, 2016; Long et al., 2016; Fig. 1). The control sites (PA control and PM control) were selected based on nearby and intact mangrove forests, with approximately 50 ha of area that had no change in NDVI after the hailstorm. Differences in the number of points chosen in each area are based on the dimension of the area impacted. Within each mangrove site, stratified points were selected (PA control = 9, PM control = 8, PA impacted 28 and PM impacted = 47) to create compound mean NDVI values, assessed through a time series. Points were evenly spaced (~250 m), avoiding transition pixels (e.g. those near water or adjacent pastures) to prevent estimation biases (Fig. 1). The time series for the impacted sites were normalized in relation to their respective control site data to remove general oscillations, such as the seasonal natural fluctuations. Absolute NDVI showed values between 0.0 and 0.5, while the normalized series was scaled from 0.0 to 1.0.

Pixels of the mangrove forest images were classified based on their NDVI values related to the ground reference of impacted (PA impacted and PM impacted) and control sites (PA control and PM control). NDVI changes were then used to classify mangrove health into four levels: i) Intact mangrove, with relative NDVI >75% of natural status; ii) Slightly impacted, with relative NDVI between 75% and 50% of natural forests; iii) moderately impacted, with relative NDVI between 50% and 25% of natural forests; and iv) severely impacted with relative NDVI <25% (Long et al., 2016). The total area for each category was calculated based on sum of pixels for all images with cloud coverage <1% (13 images).

2.4. Ground truth control

A field survey was conducted at both impacted and natural sites in the estuary to validate the mangrove imagery data. The georeferenced survey sites were overlaid on the map, then the field notes, photos and videos compared with mapped damage level categories (Long et al., 2016). Six plots within each site (control and impact) were distributed along a 100 m transect after 20 m of mangrove fringe, following standard field protocols (Kauffman and Donato, 2012). In each circular plot of 7 m fixed radius, we determined mangrove height of the highest tree, species identity, number of live trees with diameter at the breast height (DBH), number of dead trees and height and density of stumps. Dead trees were defined by the absence of leaves, being classified in three classes: class 1 = tree with small branches and twigs, class 2 = absence of twigs or small branches and may have large branches and class 3 = few or no branches, mostly stand stem or broken-topped. Seedling density was determined within a 2 m radius plot. The density and diameter of downed wood was determined along four transects of 12 m (Kauffman and Donato, 2012).

2.5. Ecosystems services valuation

Monetary values of mangrove ecosystems services that were directly relevant to the study area were assessed and valued based on the Ecosystem Service Valuation Database (TEEB; Van der Ploeg and de Groot, 2010). Selected ecosystem services from the TEEB database included: i) Nursery; ii) Recreation; iii) Food (fish and crabs); iv) Climate and v) Raw materials. Ecosystem values were averaged based on countries with comparable income per capita, and from areas with similar conservation status (i.e. partially protected sites). Service values (hectare per year in US$ dollars) were then compared to total ecosystem values (TEV) from the TEEB database and from Costanza et al. (2014). The values were then adjusted in order to account for typical mangrove services existing in the PAM estuary, and to estimate the monetary loss from the impact event. Our estimates are highly conservative since we have not included potential losses from carbon emissions from mangrove degradation and we have not included other potential services from the estuarine and forested areas (e.g. water filtration, social costs; Pendleton et al., 2012).

2.6. Statistical analyses

Daily rainfall in the PAM estuary was obtained from automatic meteorological stations (ANA) and grouped monthly (mean and standard deviation) to identify the drought event. Spatial and temporal changes in mangrove forest area between the impact and control conditions were tested (Univariate ANOVA). NDVI values were analyzed between sites (impacted and control areas) and temporal scales (years and magnitude of impact). When significant, the a posteriori Tukey-Kramer test of comparison was used due to the unequal number of samples (Dunnett, 1980). Univariate ANOVA and Tukey post hoc tests were performed using SPSS v 20.0 software (IBM SPSS Statistics Inc., Chicago, IL, USA).

3. Results

3.1. El Niño, drought and hailstorm

The months preceding the hailstorm were among the driest recorded between the 2014–2016 in the PAM estuary (Supplemental Fig. S3). Rainfall during the dry season of 2016 (Jun–Aug; 27.3 ± 18.0 $mm \cdot mo^{-1}$) was, on average, 40% lower if compared to decadal historic values (66.7 ± 16.6 $mm \cdot mo^{-1}$). The drier period was also evident during the preceding (Dec–Feb 2015; 46.0 ± 26.4 $mm \cdot mo^{-1}$) and following months from the hailstorm (Dec 2016–Feb 2017, 129.6 ± 111.5 $mm \cdot mo^{-1}$), if compared to decadal 40-yr averages for the same months (155.8 ± 43.9 $mm \cdot mo^{-1}$). The years of 2015 and 2016 had the lowest rainfall of the last five decades, with a reduction of 50% and 30% in mean monthly rainfall (56.1 ± 43.6 $mm \cdot mo^{-1}$ and 78.5 ± 93.0 $mm \cdot mo^{-1}$, respectively; Supplemental Fig. S3). During the period of study, rainfall decreased by over 40% from the dry season of 2015 (66.2 ± 56.9 $mm \cdot mo^{-1}$) if compared to same period in 2016 (27.3 ± 18.0 $mm \cdot mo^{-1}$). Historical records indicate rainfall volumes of 53.0 to 97.0 $mm \cdot mo^{-1}$ during the dry season (Apr–Sep), with higher volumes (101.1 to 211.5 $mm \cdot mo^{-1}$) during the wet season (Oct–Mar; Supplemental Fig. S3). Three of the five most intense drought events in PAM estuary happened in the 21 century. Where the longest sequence of extreme dryness months happened in May to Oct 2016 (≤−2 SPI for six months; Supplemental Fig. S4; Fig. 2). From Oct 2015 to Apr 2017 all months were under moderate to extreme dryness influence. While from May to Aug 2017 SPI returns to near normal results (−1 to 1 SPI; Fig. 2). The hailstorm led to a marked change in the wind field on June, 1st, 2016. Zonal winds were negatively intensified, resulting in stronger W and S components, resulting in a shift from S-SE-SW to W winds in the day of the hailstorm (Supplemental Fig. S5).

3.2. Mangrove structure

All mangrove sites were dominated by *Rhizophora mangle* (37 $ind \cdot ha^{-1}$; 83.8%) and *Laguncularia racemosa* (7 ind·ha; 15.0%), with the tallest tree of the mangrove forests ranging from 9.8 (±2.6 m) to 17.7 (±2.3 m). Density of seedlings was lower at the impacted sites compared to the control areas (impacted = 9 (±12) $ind \cdot m^2$, control = 23 (±4) $ind \cdot m^2$), as were the total number of trees, while the total number of downed wood pieces was much higher in the impacted areas. In general, the mangroves from the control areas were composed of live trees, mostly young, while the impacted areas were mostly composed of dead trees without leaves, fallen trees connected to the root and rotten downed wood (Supplemental Table S3). The hailstorm led to sudden changes in forest structure, with a massive tree dieback in the areas affected. Mangroves from the control sites were continually dominated by live trees, whereas impacted sites were dominated by dead trees without leaves, fallen trees and rotten downed woods (Supplemental Fig. S6; Supplemental Table S3; Supplemental videos S1 and S2). Impacted sites had over 59% (PA) to 89% (PM) of dead trees after the impact if compared to control sites, with *R. mangle* forests being the most impacted overall. The number of defoliated trees increased 80-fold, while branches removed increased 5-fold.

3.3. Remote sensing

Satellite images corroborate the acute impacts of the hailstorm on the estuarine landscape. The NDVI of the impacted and control mangroves sites were significantly different (ANOVA df = 3, F = 50.586, $p = 0.000$) and corresponded to the field assessment of mangrove forest structure. Impacted mangrove sites had lower mean NDVI values (0.24 ± 0.11 PM and 0.20 ± 0.11 PA) if compared to control sites (0.39 ± 0.03 PM and 0.39 ± 0.03 PA; $p = 0.000$; Supplemental Fig. S7). The temporal changes in mangrove forest structure after the hailstorm impact was also evident, with mean NDVI of impacted sites decreasing by over 50% after the hailstorm event (0.37 ± 0.03 and 0.13 ± 0.04: before and after, respectively; $p = 0.000$), while mean NDVI of control sites remained stable at approximately 0.4. Normalized series of NDVI illustrated differences in recovery between impacted sites; the PA impacted site has increasing NDVI rates over time (0.35 to 0.47), while the PM impacted site remained close to the initial rate (0.23 to 0.24; ANOVA df = 1, F = 23.169, $p = 0.000$; Fig. 2).

Satellite imagery revealed that before the hailstorm 245 ha of mangrove forests showed some degree of impact, increasing to 756.8 ha after the event. The hailstorm suddenly impacted an area of 511.8 ha, corresponding to damage to 29.3% of the forest area within the Conservation Unit. The hailstorm led to a sudden 16-fold and 250-fold increase in mangrove forests classed as moderately or severely impacted, respectively (Table 1). Over one year after the hailstorm, the total impacted area decreased by 90.5 ha, but the severely impacted area increased by 37.4 ha, mainly at the PM impacted site (Fig. 3). Although less-impacted areas are recovering, the more impacted regions further degraded. After 15 months, the sudden massive dieback of the mangrove (severely impacted) dominated PM, while PA could be categorized as ranging from a recovery to slightly impacted (Supplemental videos S1 and S2).

3.4. Ecosystem services value

The total value of ecosystem services in the PAM estuary was estimated at over US$ 3,308,896 yr^{-1}, with highest value from nurseries (US$ 2,092,057 yr^{-1}), recreation (US$ 604,866 yr^{-1}) and food provision (US$ 346,581 yr^{-1}; Supplemental Table S4). The total ecosystem value (TEV) of the mangroves in the PAM estuary were evaluated in US$ 1895 $ha \cdot yr^{-1}$. The impacted area of 511.8 ha then represent a potential loss of ecosystem services of US$ 969,927 per year since June 2016. Food provision, nursery, climate and raw materials were likely the most direct services impacted in the area, with monetary losses up to US$ 792,624 per year.

4. Discussion

The potential effects of climate change and increasing intensity of flood and drought events and frequency of storms on mangrove forests are widely discussed in the literature (Alongi, 2008; Gilman et al., 2008;

Table 1
Area of mangrove forest in each category before (1 Jan 2016), immediately after the storm (11 Jul 2016) and one year after the impact (31 Aug 2017). Slightly impacted (25–50% NDVI loss), Moderately (50–75% NDVI loss), Heavily impacted (>75% NDVI loss).

	1 Jan 2016		11 Jul 2016		31 Aug 2017	
	ha	(% area)	ha	(% area)	ha	(% area)
Slightly impacted	221.7	(12.7)	256.3	(14.7)	256.1	(14.7)
Moderately impacted	22.8	(1.3)	365.1	(20.9)	237.4	(13.6)
Severely impacted	0.5	(0.0)	135.4	(7.8)	172.8	(9.9)
Total impacted	245.0	(14.0)	756.8	(43.4)	666.3	(38.2)
Not impacted	1501.0	(86.0)	989.2	(56.7)	1079.7	(61.8)

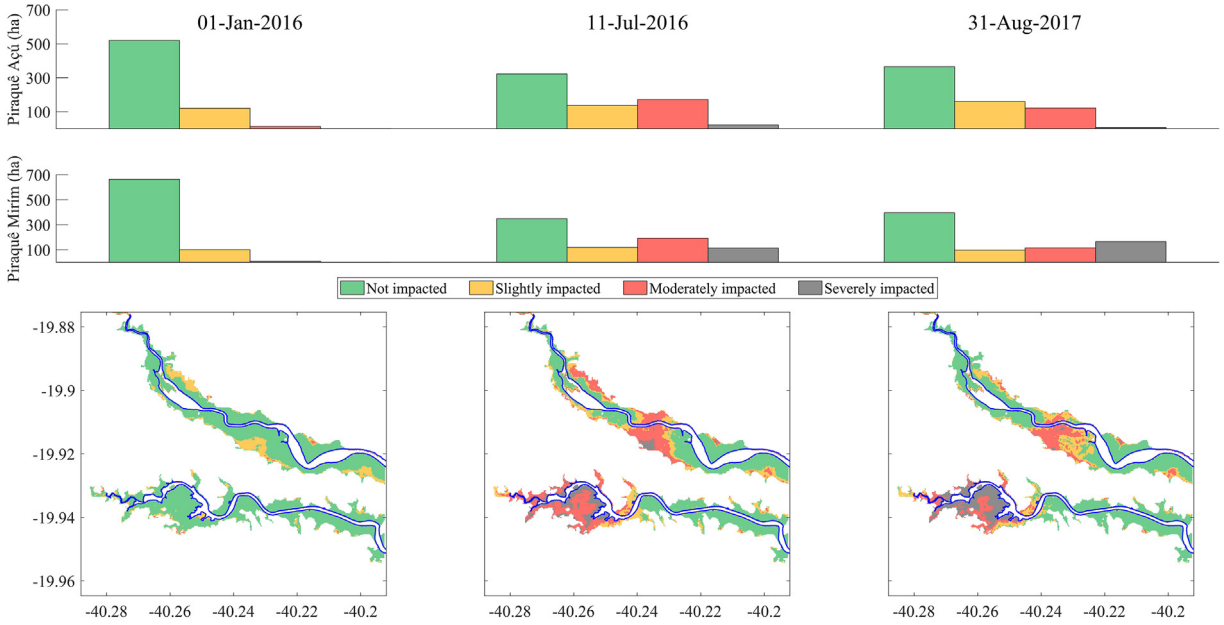

Fig. 3. Map and area bars of impacted and non-impacted mangrove areas in the PAM before and after the storm. Not impacted (green); B. Slightly impacted (yellow); C. Moderately impacted (red); and D. Severely impacted (gray) forests.

Dai, 2013). In estuaries, drought anomalies can change the salt balance by increasing evapotranspiration or decreasing the fresh water influx (McLusky and Elliott, 2004; Dai, 2013; MacKay et al., 2010). In the present study, a drastic reduction in rainfall rates occurred during a very strong El Niño, the highest this century (>2.0; ggweather, 2017), observed in the Caribbean during this same period (Herrera and Ault, 2017). El Niño influences the local climate around the world and leads to increased drought risk (Grimm et al., 1998; Dai, 2013), influenced by the Tropical Pacific and North Atlantic oceans (Herrera and Ault, 2017). In the South Atlantic, intense storms such as hurricanes and typhoons, which can be of large scale and intensity, are less threatening to coastal ecosystems; localized climatic events, however, may create extreme weather conditions, resulting in immediate loss of trees followed by recovery of that forest cover over time (Macamo et al., 2016; Long et al., 2016). Hailstorms may occur during meteorological instability and high humidity, leading to intense winds that will keep the hail in the atmosphere until it is heavy enough to fall to the ground (Foote, 1984; Wallace and Hobbs, 2006). Wind shear defines storm intensity and promotes hail formation (Huschke, 1959; Modahl, 1969). In the hailstorm that impacted PAM mangroves, the rapid changes in wind direction likely contributed to the formation and occurrence of the hail that physically defoliated and downed mangrove trees. The Eastern Brazil Marine Ecoregion is under decadal atmospheric warming and will likely experience an increase in drought periods from global warming effects (Dai, 2013; Bernardino et al., 2015). El Niño years also contribute to drier and longer periods with higher atmospheric accumulated kinetic energy (AKE), which may increase the potential damage from hailstorms during warm years (Allen et al., 2015; Brimelow et al., 2017). The potential damage that low to moderate disturbances may have on mangrove forests in semi-arid areas and the likelihood that some of these events may become frequent and more intense highlight the need to understand and monitor these events.

Hailstorm impacts on mangrove forests can cause bark damage, loss of floral buds and fruits and major canopy defoliation (Houston, 1999; Clarke, 1992). The hailstorm damage to the PAM estuary impacted nearly 30% of the mangrove forests, which has no comparable precedent found in literature for South America. Moreover, typical storm effects were observed in impacted forests, with widespread tree defoliation and many individuals being knocked down facing the same direction, evidence that strong winds caused sudden uprooting and death. Storm intensity and forest exposure may be important to the scale of impact and mangrove regrowth (Supplemental Table S5). The continued degradation after the hailstorm suggests that environmental stress persisted in some areas of PAM estuary, likely impairing mangrove recovery. While the recovery area (PA) evidence seedling growth and regeneration of fresh leaves in some areas. For example, mangrove recovery after hailstorm and hurricanes has a recovery period longer than one year, as observed at the PM site (Roth, 1992; Houston, 1999; Smith III et al., 2009; Long et al., 2016), but we detected a minor recovery of mangrove forests in some areas of PA 15 months after the hailstorm. The lack of recovery was evident from satellite imagery (increase in severely impacted area; PM), by an absence of seedling growth and no regeneration of fresh leaves in the impacted sites.

The potential loss of mangrove forests due to increased thermal stress in association with other effects have only been recently documented (Silliman et al., 2005; Duke et al., 2017). Higher salinity and thermal stress may lead to slower tree growth and lower leaf gas exchange as a result of diminished stomatal openings, as well as lower seedling survival (Farquhar et al., 1982; Lin and Sternberg, 1992). The frequency and intensity of El Niño events are particularly concerning, since changes in temperature and precipitation regimes are key factors for mangrove ecosystem transformations (Gabler et al., 2017; Feher et al., 2017). Survival and recovery of mangroves are influenced by soil salinization during drought events, where the reduction in freshwater input may also impair mangrove health and recovery from water stress (Cintrón et al., 1978; Ball, 1988; Houston, 1999; MacKay et al., 2010). PM previously displayed hypersaline conditions, an important driver for mangrove forest transformation into other ecosystems, because trees cannot tolerate such an increase in salinity for long periods (Osland et al., 2016; Lovelock et al., 2016). The El Niño years of 2015–2016 were among the warmest and driest in the last few decades globally. In 2015, the decrease in rainfall volume was 50% lower compared to a 40-yr average in the PAM estuary, prior to the hailstorm (>2.0 SST; Bernardino et al., 2015; ggweather, 2017). We hypothesize that the limited mangrove recovery and further degradation at some sites after the hailstorm event in the PAM estuary was likely influenced by mild drought periods (Dai, 2013; Duke et al., 2017). *Rhizophora mangle* were more sensitive to salinization of the estuary compared to *Laguncularia racemosa* and *Avicennia schaueriana*, which can accumulate and secrete salt, regulating the salt balance (Ball, 1988; Parida and

Jha, 2010). The salinity stress, ultimately caused by the mild drought condition of 2014–2016, was a major factor that accentuated the overall impact of the hailstorm in the PAM estuary (see Houston, 1999).

We have not assessed potential impacts of sea-level changes or any biological pests in our study area, but these effects may play a significant role in mangrove survival over large scales (Silliman et al., 2005; Alongi, 2008; Duke et al., 2017). An improved monitoring of sea-level oscillation and long-term changes in temperature, precipitation, water salinity and oxygenation would greatly benefit management of such estuarine ecosystems given climate change (IPCC, 2001).

Economic impacts of mangrove losses regionally include essential services such as food provision through fishing and manual crab captures, and also carbon sequestration by forests and soils which are not yet not a source of revenue regionally. Many estuarine and marine fish species (e.g. *Lutjanus* spp.) use the PAM mangroves as habitat, nursery and feeding grounds (Vilar et al., 2013). Other commercially important species (e.g. *Callinectes* spp.) have larval settlement and recruits on *Rhizophora mangle* roots (Johnston and Caretti, 2017), supporting that nursery services are essential to this area. The potential economic losses from mangrove ecosystem services in the PAM estuary of US$ 1895 $ha \cdot yr^{-1}$ are within the total ecosystem values (TEV) of mangroves in the Caribbean and Latin America (Van der Ploeg and de Groot, 2010). The TEV of the PAM mangroves are likely a lower estimate since many important ecosystems services have not been estimated in the area, including for example water filtration, social values and CO_2 and CH_4 emissions from land use change (Costanza et al., 2014; Kauffman et al., 2016, 2018). Losses in the impacted area also included the extraction of raw materials by traditional populations such as wood for construction, tannin extraction and fishnets (Santos and Lana, 2017). The essential food provision from fishing and crab captures to fishers (Cortes et al., 2014) may be the most relevant monetary impact threatening their subsistence, and may account for over 50% of the municipality's gross production within 2 years. The total economic losses from this impact (U$$ 969,927) are significantly lower than US$ 33 million per year that would be obtained by using ecological values of Costanza et al. (2014). Although the values of many ecosystems services were not assessed in the PAM mangroves, the marked differences in those estimates highlight the need to develop and expand local and regional assessments of ecosystem services in light of several ecosystem impacts that mangroves and estuaries are experiencing in Brazil (Gomes et al., 2017; Bernardino et al., 2018).

This is the first evidence of extreme weather impacts on mangrove forests in South America, which caused massive tree dieback and continuing degraded conditions 15 months after the impact. As observed in other coastal wetlands under potential thermal and drought effects, mangrove recovery is likely being impaired by physiological stress of adults and seedlings. Over one year after the hailstorm, ecosystem impacts on PAM mangroves persist and have brought great uncertainty to local populations that have suffered the most economic losses. Our results demonstrate the unique importance of climate change adaptation actions and coastal monitoring throughout the extensive mangrove forests in Brazil, which have great social, economic and climatic value.

Supplementary data to this article can be found online at https://doi.org/10.1016/j.scitotenv.2018.02.068.

Conflict of interest

The authors declare no actual or potential conflict of interest.

Contribution

RNS, LEOG and AFB participated in sampling, analyzed data and wrote the manuscript. All authors have approved the final article.

Acknowledgements

We would like to thank A. Mazzuco, F. Cortes (IDAF-ES) and P·Pimentel for contributing to the data, photos and videos and to the Aracruz Municipal Administration (PMA-ES), for field support for this work. AFB was supported by CNPq (grant 441243/2016-9) and FAPES (grant 79054684/17). LEOG was supported by a CNPq PELD-HCES scholarship. This is a PELD-HCES contribution # 002.

References

Allen, J.T., Tippett, M.K., Sobel, A.H., 2015. Influence of the El Niño/Southern Oscillation on tornado and hail frequency in the United States. Nat. Geosci. 8:278–283. https://doi.org/10.1038/NGEO2385.

Alongi, D.M., 2008. Mangrove forests: resilience, protection from tsunamis, and responses to global climate change. Estuar. Coast. Shelf Sci. 76:1–13. https://doi.org/10.1016/j.ecss.2007.08.024.

Alongi, D.M., 2012. Carbon sequestration in mangrove forests. Carbon Manage. 3: 313–322. https://doi.org/10.4155/cmt.12.20.

Alvares, C.A., Stape, J.L., Sentelhas, P.C., Gonçalves, J.L.M., Sparovek, G., 2013. Koppen's climate classification map for Brazil. Metereologische Zeitschrift 22:711–728. https://doi.org/10.1127/0941-2948/2013/0507.

Ball, M., 1988. Ecophysiology of mangroves. Trees 2:129–142. https://doi.org/10.1007/BF00196018.

Bernardino, A.F., Netto, S.A., Pagliosa, P.R., Barros, F., Christofoletti, R.A., Rosa-Filho, J.S., Colling, J., Lana, P.C., 2015. Predicting ecological changes on benthic estuarine assemblages through decadal climate trends along Brazilian Marine Ecoregions. Estuar. Coast. Shelf Sci. 166:74–82. https://doi.org/10.1016/j.ecss.2015.05.021.

Bernardino, A.F., Gomes, L.E.O., Hadlich, H.L., Andrades, R., Correa, L.B., 2018. Mangrove clearing impacts on macrofaunal assemblages and benthic food webs in a tropical estuary. Mar. Pollut. Bull. 126:228–235. https://doi.org/10.1016/j.marpolbul.2017.11.008.

Brimelow, J.C., Burrows, W.R., Hanesiak, J.M., 2017. The changing hail threat over North America in response to anthropogenic climate change. Nat. Clim. Chang. 7:516–522. https://doi.org/10.1038/NCLIMATE3321.

Cahoon, D.R., Hensel, P., Rybczyk, J., McKee, K.L., Proffitt, C.E., Perez, B.C., 2003. Mass tree mortality leads to mangrove peat collapse at bay islands, Honduras after hurricane mitch. J. Ecol. 91:1093–1105. https://doi.org/10.1046/j.1365-2745.2003.00841.x.

Cintrón, G., Lugo, A.E., Pool, D.J., Morris, G., 1978. Mangroves of arid environments in Puerto-Rico and adjacent islands. Biotropica 10 (2):110–121. https://doi.org/10.2307/2388013.

Clarke, P.J., 1992. Predispersal mortality and fecundity in the grey mangrove (*Avicennia marina*) in southeastern Australia. Aust. J. Ecol. 17:161–168. https://doi.org/10.1111/j.1442-9993.1992.tb00794.x.

Cortes, L.H.O., Zappes, C.A., Di Beneditto, A.M., 2014. Extração e cadeia produtiva do caranguejo-uça no norte do Rio de Janeiro. Boletim do Instituto de Pesca SP 40 (4), 639–656.

Costanza, R., de Groot, R., Sutton, P., van der Ploeg, S., Anderson, S.J., Kubiszewski, I., Farber, S., Turner, R.K., 2014. Changes in the global value of ecosystem services. Glob. Environ. Chang. 26:152–158. https://doi.org/10.1016/j.gloenvcha.2014.04.002.

Dai, A., 2013. Increasing drought under global warming in observations and models. Nat. Clim. Chang. 3:171. https://doi.org/10.1038/nclimate1811.

Donato, D.C., Kauffman, J.B., Murdiyarso, D., Kurnianto, S., Stidham, M., Kanninen, M., 2011. Mangroves among the most carbon-rich forests in the tropics. Nat. Geosci. 4: 293–297. https://doi.org/10.1038/ngeo1123.

Doney, S.C., Ruckelshaus, M., Duffy, J.E., Barry, J.P., Chan, F., Englidh, C.A., Galindo, H. M., Grebmeier, J.M., Hollowed, A.B., Knowlton, N., Polovina, J., Rabalais, N.N., Sydeman, W.J., Talley, L.D., 2012. Climate change impacts on marine ecosystems. Annu. Rev. Mar. Sci. 4:11–37. https://doi.org/10.1146/annurev-marine-041911-111611.

Duke, N.C., Kovacs, J.M., Griffths, A.D., Preece, L., Hill, D.J.E., van Oosterzee, P., Mackenzie, J., Morning, H.S., Burrows, D., 2017. Large-scale dieback of mangroves in Australia's Gulf of Carpentaria: a severe ecosystem response, coincidental with an unusually extreme weather event. Mar. Freshw. Res. 68: 1816–1829. https://doi.org/10.1071/MF16322.

Dunnett, C.W., 1980. Pairwise multiple comparisons in the homogeneous variance, unequal sample size 394 case. J. Am. Stat. Assoc. 372, 789–795.

Farquhar, G.D., Ball, M.C., von Caemmerer, S., Roksandic, Z., 1982. Effects of salinity and humidity on 6% values of halophytes evidence for diffusional isotope fractionation determined by the ratio of intercellular/atmospheric C02 under different environmental conditions. Oecologia 52:121–124. https://doi.org/10.1007/BF00349020.

Feher, L.C., Osland, M.J., Griffith, K.T., Grace, J.B., Howard, R.J., Stagg, C.L., Enwright, N.M., Krauss, K.W., Gabler, C.A., Day, R.H., Rogers, K., 2017. Linear and nonlinear effects of temperature and precipitation on ecosystem properties in tidal saline wetlands. Ecosphere 8, e01956. https://doi.org/10.1002/ecs2.1956.

Foote, G.B., 1984. A study of hail growth utilizing observed storm conditions. J. Clim. Appl. Meteorol. 23, 84–101.

Gabler, C.A., Osland, M.J., Grace, J.B., Stagg, C.L., Day, R.H., Hartley, S.B., Enwright, N.M., From, A.S., McCoy, M.L., McLeod, J.L., 2017. Macroclimatic change expected to transform coastal wetland ecosystems this century. Nat. Clim. Chang. 7:142–147. https://doi.org/10.1038/NCLIMATE3203.

ggweather (Golden Gate Weather Services Comparative Climatic Data), 2017. Website:. http://ggweather.com/enso/oni.htm, Accessed date: 5 October 2017.

Gilman, E.L., Ellison, J.C., Duke, N.C., Field, C., 2008. Threats to mangroves from climate change and adaptation options: a review. Aquat. Bot. 89:237–250. https://doi.org/10.1016/j.aquabot.2007.12.009.

Giri, C., Ochieng, E., Tieszen, L.L., Zhu, Z., Singh, A., Loveland, T., Masek, J., Duke, N., 2010. Status and distribution of mangrove forests of the world using earth observation satellite data. Glob. Ecol. Biogeogr. 20:154–159. https://doi.org/10.1111/j.1466-8238.2010.00584.x.

Gomes, L.E.O., Correa, L.B., Sá, F., Neto, R.R., Bernardino, A.F., 2017. The impacts of the Samarco mine tailing spill on the Rio Doce estuary, Eastern Brazil. Mar. Pollut. Bull. 120:28–36. https://doi.org/10.1016/j.marpolbul.2017.04.056.

Grimm, A.M., Ferraz, S.E.T., Gomes, J., 1998. Rainfall anomalies in Southern Brazil associated with El Niño and La Niña events. J. Clim. 11:2863–2880. https://doi.org/10.1175/1520-0442(1998)011<2863:PAISBA>2.0.CO;2.

Herrera, D., Ault, T., 2017. Insights from a new high-resolution drought atlas for the Caribbean spanning 1950 to 2016. J. Clim. 30:7801–7825. https://doi.org/10.1175/JCLI-D-16-0838.1.

Holben, B.N., 1986. Characteristics of maximum-value composite images from temporal AVHRR data. Int. J. Remote Sens. 7:1417–1434. https://doi.org/10.1080/01431168608948945.

Houston, W.A., 1999. Severe hail damage to mangroves at Port Curtis, Australia. Mangrove Salt Marshes 3:29–40. https://doi.org/10.1023/A:1009946809787.

Huschke, R.E., 1959. Glossary of Meteorology. Amer. Meteor. Soc., Boston (638 pp.).

Ibharim, N.A., Mustapha, M.A., Lihan, T., Mazlan, A.G., 2015. Mapping mangrove changes in the Matang Mangrove Forest using multi temporal satellite imageries. Ocean Coast. Manag. 114:64–76. https://doi.org/10.1016/j.ocecoaman.2015.06.005.

IPCC, 2001. In: Houghton, J.T., Ding, Y., Griggs, D.J., Noguer, M., van der Linden, P.J., Dai, X., Maskell, K., Johnson, C.A. (Eds.), Climate Change 2001: The Scientific Basis. Contribution of Working Group I to the Third Assessment Report of the Intergovernmental Panel on Climate Change. Cambridge University Press, Cambridge, United Kingdom and New York, NY, USA (881 pp.).

Johnston, C.A., Caretti, O.N., 2017. Mangrove expansion into temperate marshes alters habitat quality for recruiting *Callinectes* spp. Mar. Ecol. Prog. Ser. 573:1–14. https://doi.org/10.3354/meps12176.

Jones, R., 2015. Quantifying extreme weather event impacts on the northern Gulf Coast using Landsat imagery. J. Coast. Res. 31:1229–1240. https://doi.org/10.2112/JCOASTRES-D-14-00065.

Kalnay, E., Kanamitsu, M., Kistler, R., Collins, W., Deaven, D., Gandin, L., Iredell, M., Saha, S., White, G., Woollen, J., Zhu, Y., Chelliah, M., Ebisuzaki, W., Higgins, W., Janowiak, J., Mo, K.C., Ropelewski, C., Wang, J., Leetmaa, A., Reynolds, R., Jenne, R., Joseph, D., 1996. The NCEP/NCAR 40-year reanalysis project. Bull. Am. Meteorol. Soc. 77:437–472. https://doi.org/10.1175/1520-0477(1996)077<0437:TNY RP>2.0.CO;2.

Kauffman, J.B., Donato, D.C., 2012. Protocols for the measurement, monitoring and reporting of structure, biomass and carbon stocks in mangrove forests. Working Paper 86. CIFOR, Bogor, Indonesia (50 pp.).

Kauffman, J.B., Trejo, H.H., Jesus Garcia, M.C., Heider, C., Contreras, W.M., 2016. Carbon stocks of mangroves and losses arising from their conversion to cattle pastures in the Pantanos de Centla, Mexico. Wetl. Ecol. Manag. 24:203–216. https://doi.org/10.1007/s11273-015-9453-z.

Kauffman, J.B., Arifanti, V.B., Bernardino, A.F., Ferreira, T.O., Murdiyarso, D., Cifuentes, M., Norfolk, J., 2018. And details for land-use change carbon footprints arise from quantitative and replicated studies. Front. Ecol. Environ. 1749:12–13. https://doi.org/10.1002/fee.1749.

Kristensen, E., Flindt, M.R., Ulomi, S., Borges, A.V., Abril, G., Bouillon, S., 2008. Emission of CO2 and CH4 to the atmosphere by sediments and open waters in two Tanzanian mangrove forests. Mar. Ecol. Prog. Ser. 370:53–67. https://doi.org/10.3354/meps07642.

Lin, G., Sternberg, L., 1992. Effect of growth form, salinity, nutrient and sulfide on photosynthesis, carbon isotope discrimination and growth of Red Mangrove (*Rhizophora mangle* L.). Funct. Plant Biol. 19:509–517. https://doi.org/10.1071/PP9920509.

Long, J., Giri, C., Primavera, J., Trivedi, M., 2016. Damage and recovery assessment of the Philippines' mangroves following Super Typhoon Haiyan. Mar. Pollut. Bull. 109: 734–743. https://doi.org/10.1016/j.marpolbul.2016.06.080.

Lovelock, C.E., Krauss, K.W., Osland, M.J., Reef, R., Ball, M.C., 2016. The physiology of mangrove trees with changing climate. Trop. Tree Physiol. 6:149–179. https://doi.org/10.1007/978-3-319-27422-5_7.

Macamo, C.C.F., Massuanganhe, E., Nicolau, D.K., Bandeira, S.O., Adams, J.B., 2016. Mangrove's response to cyclone Eline (2000): what is happening 14 years later. Aquat. Bot. 134:10–17. https://doi.org/10.1016/j.aquabot.2016.05.004.

MacKay, F., Cyrus, D., Russell, K.L., 2010. Macrobenthic invertebrate responses to prolonged drought in South Africa's largest estuarine lake complex. Estuar. Coast. Shelf Sci. 86:553–567. https://doi.org/10.1016/j.ecss.2009.11.011.

Marengo, J.A., Ambrizzi, T., da Rocha, R.P., Alves, L.M., Cuadra, S.V., Valverde, M.C., Torres, R.R., Santos, D.C., Ferraz, S.E.T., 2010. Future change of climate in South America in the late twenty-first century: intercomparison of scenarios from three regional climate models. Clim. Dyn. 35, 1073–1097.

MATLAB 9.0. The MathWorks Inc., Natick, MA.

McKee, T.B., Doesken, N.J., Kleist, J., 1993. The relationship of drought frequency and duration to time scales. Eighth Conference on Applied Climatology, pp. 17–22.

McKee, K.L., Mendelssohn, I.A., Materne, M.D., 2004. Acute salt marsh dieback in the Mississippi River deltaic plain: a drought-induced phenomenon? Glob. Ecol. Biogeogr. 13:65–73. https://doi.org/10.1111/j.1466-882X.2004.00075.x.

McLeod, E., Salm, R., 2006. Managing Mangroves for Resilience to Climate Change. IUCN, Gland, Switzerland.

Mcleod, E., Chmura, G.L., Bouillon, S., Salm, R., Bjork, M., Duarte, C.M., Lovelock, C.E., Schlesinger, W.H., Silliman, B.R., 2011. A blueprint for blue carbon: towards an improved understanding of the role of vegetated coastal habitats in sequestering CO2. Front. Ecol. Environ. 9:552–560. https://doi.org/10.1002/fee.1491.

McLusky, D.S., Elliott, M., 2004. The Estuarine Ecosystem: Ecology, Threats, and management. Oxford University Press, New York 214pp. https://doi.org/10.1016/j.marpolbul.2014.03.049.

Modahl, A.C., 1969. The Influence of Vertical Wind Shear on Hailstorm Development and Structure. Colorado State University, Colorado (63 pp.).

Moreira, E.E., Coelho, C.A., Paulo, A.A., Pereira, L.S., Mexia, J.T., 2008. SPI-based drought category prediction using loglinear models. J. Hydrol. 354:116–130. https://doi.org/10.1016/j.jhydrol.2008.03.002.

Osland, M.J., Enwright, N.M., Day, R.H., Gabler, C.A., Stagg, C.L., Grace, J.B., 2016. Beyond just sea-level rise: considering macroclimatic drivers within coastal wetland vulnerability assessments to climate change. Glob. Chang. Biol. 22:1–11. https://doi.org/10.1111/gcb.13084.

Osland, M.J., Feher, L.C., Griffith, K.T., Cavanaugh, K.C., Enwright, N.M., Day, R.H., Stagg, C.L., Krauss, K.W., Howard, R.J., Grace, J.B., Rogers, K., 2017. Climatic controls on the global distribution, abundance, and species richness of mangrove forests. Ecol. Monogr. 87: 341–359. https://doi.org/10.1002/ecm.1248.

Parida, A.K., Jha, B., 2010. Salt tolerance mechanisms in mangroves: a review. Trees 24: 199–217. https://doi.org/10.1007/s00468-010-0417-x.

Pendleton, L., Donato, D.C., Murray, B.C., Crooks, S., Jenkins, W.A., Sifleet, S., Craft, C., Fourqurean, J.W., Kauffman, J.B., Marba, N., Megonigal, P., Pidgeon, E., Herr, D., Gordon, D., Baldera, A., 2012. Estimating global "blue carbon" emissions from conversion and degradation of vegetated coastal ecosystems. PLoS One 7, e43542. https://doi.org/10.1371/journal.pone.0043542.

Pettorelli, N., 2013. The Normalized Difference Vegetation Index. OUP, Oxford (224 pp.).

PMA (Prefeitura Municipal de Aracruz), 2013. Lei n° 3.739 – Altera a categoria da Unidade de Conservação Reserva Ecológica dos Manguezais Piraquê-Açú e Piraquê-Mirím para Reserva de Desenvolvimento Sustentável Municipal Piraquê-Açú e Piraquê-Mirím no município de Aracruz, Estado do Espírito Santo, e das outras providências (5 pp.).

Queiroz, S.Q., Rossi, S., Calvet-Mir, L., Ruiz-Mallén, I., García-Betorz, S., Salvà-Prat, J., Meireles, A.J.A., 2017. Neglected ecosystem services: highlighting the socio-cultural perception of mangroves in decision-making processes. Ecosyst. Serv. 26:137–145. https://doi.org/10.1016/j.ecoser.2017.06.013.

Roth, L.C., 1992. Hurricanes and mangrove regeneration: effects of hurricane Joan, October 1988, on the vegetation of Isla del Venado, Bluefields, Nicaragua. Biotropica 24, 375–384.

Rouse, J.W., Haas, R.H., Scheel, J.A., Deering, D.W., 1974. Monitoring vegetation systems in the great plains with ERTS. Proceedings, 3rd Earth Resource Technology Satellite (ERTS) Symposium, 1, pp. 48–62.

Santos, N.M., Lana, P., 2017. Present and past uses of mangrove wood in the subtropical Bay of Paranaguá (Paraná, Brazil). Ocean Coast. Manag. 148:97–103. https://doi.org/10.1016/j.ocecoaman.2017.07.003.

Schaeffer-Novelli, Y., Soriano-Sierra, E.J., Vale, C.C., Bernini, E., Rovai, A.S., Pinheiro, M.A.A., Schmidt, A.J., Almeida, R., Júnior, C.C., Menghini, R.P., Martinez, D.I., Abuchahla, G.M. O., Cunha-Lignon, M., Charlier-Sarubo, S., Shirazawa-Freitas, J., Cintrón-Molero, G., 2016. Climate changes in mangrove forests and salt marshes. Braz. J. Oceanogr. 64: 37–52. https://doi.org/10.1590/S1679-875920160919064sp2.

Silliman, B.R., Koppel, J.D., Bertness, M.D., Stanton, L.E., Mendelssohn, I.A., 2005. Drought, snails, and large-scale die-off of southern US salt marshes. Science 310:1803–1806. https://doi.org/10.1126/SCI ENCE.1118229.

Smith III, T.J., Anderson, G.H., Balentine, K., Tiling, G., Ward, G.A., Whelan, K.R.T., 2009. Cumulative impacts of hurricanes on Florida mangrove ecosystems: sediment deposition, storm surges and vegetation. Wetlands 29:24–34. https://doi.org/10.1672/08-40.1.

Tamura, M., Kikushima, K., 2008. Extraction of mangrove forests using a satellite image and a digital elevation model. Proc. SPIE 7104, Remote Sensing for Agriculture, Ecosystems, and Hydrology X:p. 710403 https://doi.org/10.1117/12.799341.

U.S. Geological Survey, 2017a. EarthExplorer. Website. *https://earthexplorer.usgs.gov*, Accessed date: 10 July 2017.

U.S. Geological Survey, 2017b. Landsat 8 Pre-Collection Quality Assessment Band. Website. https://landsat.usgs.gov/qualityband, Accessed date: 19 July 2017.

Underwood, A.J., 1992. Beyond BACI: the detection of environmental impacts on populations in the real, but variable, world. J. Exp. Mar. Biol. Ecol. 161:145–178. https://doi.org/10.1016/0022-0981(92)90094-Q.

Van der Ploeg, S., de Groot, R.S., 2010. The TEEB Valuation Database-a searchable database of 1310 estimates of monetary values of ecosystem services. Foundation for Sustainable Development, Wageningen, the Netherlands.

Vilar, C.C., Joyeux, J., Giarrizzo, T., Spach, H.L., Vieira, J.P., Vaske-Junior, T., 2013. Local and regional ecological drivers of fish assemblages in Brazilian estuaries. Mar. Ecol. Prog. Ser. 485:181–197. https://doi.org/10.3354/meps10343.

Wallace, J.M., Hobbs, P.V., 2006. Atmospheric Science: An Introductory Survey. 2nd ed. Academic Press, Burlington, MA (483 pp.).

Yengoh, G.T., Dent, D., Olsson, L., Tengberg, A.E., Tucker III, C.J., 2015. Use of the Normalized Difference Vegetation Index (NDVI) to Assess Land Degradation at Multiple Scales: Current Status, Future Trends, and Practical Considerations. Springer (110 pp.).